AGU ADVANCING EARTH AND SPACE SCIENCES

Geophysical Research Letters

RESEARCH LETTER
10.1029/2024GL108459

Insights Into Changing Interglacial Conditions in Subarctic Canada From MIS 11 Through MIS 5e From Seasonally Resolved Speleothem Records

Cameron J. Batchelor[1], David McGee[1], Jeremy D. Shakun[2], Jon Woodhead[3], Adam B. Jost[1], Sarah Arnold[4], Greg Horne[5], Christopher W. Kinsley[6], and Markey Freudenburg-Puricelli[1]

[1]Department of Earth, Atmospheric and Planetary Sciences, Massachusetts Institute of Technology, Cambridge, MA, USA, [2]Department of Earth and Environmental Sciences, Boston College, Chestnut Hill, MA, USA, [3]School of Geography, Earth and Atmospheric Sciences, University of Melbourne, Parkville, VIC, Australia, [4]Parks Canada, Fort Simpson, NT, Canada, [5]Jasper National Park, Jasper, AB, Canada, [6]Berkeley Geochronology Center, Berkeley, CA, USA

Key Points:

- Long high-latitude terrestrial climate records are rare in the Northern Hemisphere
- High-latitude speleothems can provide ultra-high-resolution climate records beyond the reach of Greenland ice cores
- Mean oxygen isotopes of Arctic and subarctic speleothems likely are controlled by annual ground thaw durations

Supporting Information:

Supporting Information may be found in the online version of this article.

Correspondence to:

C. J. Batchelor,
cambatch@mit.edu

Citation:

Batchelor, C. J., McGee, D., Shakun, J. D., Woodhead, J., Jost, A. B., Arnold, S., et al. (2024). Insights into changing interglacial conditions in subarctic Canada from MIS 11 through MIS 5e from seasonally resolved speleothem records. *Geophysical Research Letters*, *51*, e2024GL108459. https://doi.org/10.1029/2024GL108459

Received 25 JAN 2024
Accepted 10 MAR 2024

Author Contributions:

Conceptualization: Cameron J. Batchelor, David McGee, Jeremy D. Shakun, Jon Woodhead
Formal analysis: Cameron J. Batchelor, David McGee, Jeremy D. Shakun, Jon Woodhead
Funding acquisition: Cameron J. Batchelor, David McGee, Jeremy D. Shakun
Investigation: Cameron J. Batchelor, David McGee, Jeremy D. Shakun, Jon Woodhead
Methodology: Cameron J. Batchelor, Adam B. Jost, Sarah Arnold, Greg Horne, Christopher W. Kinsley, Markey Freudenburg-Puricelli
Resources: Sarah Arnold, Greg Horne

Abstract High-resolution records from past interglacial climates help constrain future responses to global warming, yet are rare. Here, we produce seasonally resolved climate records from subarctic-Canada using micron-scale measurements of oxygen isotopes ($\delta^{18}O$) in speleothems with apparent annual growth bands from three interglacial periods—Marine Isotope Stages (MIS) 11, 9, and 5e. We find 3‰ lower $\delta^{18}O$ values during MIS 11 than MIS 5e, despite MIS 11 likely being warmer. We explore controls on high-latitude speleothem $\delta^{18}O$ and suggest low MIS 11 $\delta^{18}O$ values reflect greater contribution of cold-season precipitation to dripwater from longer annual ground thaw durations. Other potential influences include changes in precipitation source and/or increased fraction of cold-season precipitation from diminished sea ice in MIS 11. Our study highlights the potential for high-latitude speleothems to yield detailed isotopic records of Northern Hemisphere interglacial climates beyond the reach of Greenland ice cores and offers a framework for interpreting them.

Plain Language Summary Few climate records pre-dating the last ice age exist from high-latitude North America, which inhibits our understanding of how regions with permafrost responded to past warming and how they might change in the future. Here, we help fill this data gap by using six speleothems (cave mineral deposits) from a cave in the Northwest Territories, Canada to produce climate records that span thousands of years during former warm periods of Earth's history. We find that speleothems that grew during an exceptionally warm super-interglacial period 400,000 years ago have 3‰ lower oxygen isotope ($\delta^{18}O$) values compared to those that grew during a likely cooler interglacial 125,000 years ago. We explore potential explanations for the difference in $\delta^{18}O$ across interglacials, and suggest that lower $\delta^{18}O$ values during warmer periods reflect greater infiltration of cool-season precipitation with longer annual ground thaw durations. This study highlights the importance of high-latitude speleothems to provide detailed climate records beyond the range available from Greenland ice cores.

1. Introduction

The high-latitudes of the Northern Hemisphere are warming at three to four times the rate of the rest of the planet in response to human-driven increases in atmospheric greenhouse gases, raising concern that the region is approaching tipping points related to permafrost, sea ice, and the Greenland ice sheet (Pörtner et al., 2022). Past warm periods in Earth's history—including Pleistocene interglacials—offer valuable opportunities for gauging the responses of Arctic and subarctic regions to sustained periods of temperatures equal to or higher than present. In particular, the interglacial periods over the last 450 ka—or Marine Isotope Stages (MIS) 11, 9, 7, and 5 (Lisiecki & Raymo, 2005)—provide an opportunity to constrain variability during a time when some regions of Earth's surface may have been warmer than today.

Unfortunately, high-latitude Northern Hemisphere terrestrial climate records from the last four interglacial periods are rare to nonexistent, due primarily to erosional processes that limit preservation of continuous climate archives. Greenland ice cores have long provided key records of high-latitude climate in the Northern Hemisphere (e.g., NGRIP members, 2004); however, they extend only back to the Last Interglacial period (MIS 5e, ~125 ka). More recently, foundational records extending through the Pleistocene have been developed from sediments

Writing – original draft: Cameron J. Batchelor, David McGee, Jeremy D. Shakun, Jon Woodhead
Writing – review & editing: Cameron J. Batchelor, David McGee, Jeremy D. Shakun, Jon Woodhead

recovered from Lake El'gygytgyn, NE Russia, where data suggest summer temperatures 4–5°C above modern during so-called "super interglacials" (Melles et al., 2012), including MIS 11. Climate records off southern Greenland, however, suggest MIS 9 (Irvalı et al., 2020) or MIS 5e (Cluett & Thomas, 2021) were exceptionally warm. A recent temperature reconstruction suggests global warmth was similar during MIS 11 and MIS 5e (Clark et al., 2024). These studies highlight discrepancies among records and regions on which interglacial was warmest, and it remains unclear how climates during past interglacials affected other high-latitude continental regions.

The spatial and temporal limitations of existing records have begun to be addressed through the study of Arctic and subarctic speleothems. Speleothems constitute valuable environmental archives, as they can be precisely dated (Cheng et al., 2013) and their oxygen isotope ratios ($\delta^{18}O$) reflect a combination of cave temperature and $\delta^{18}O$ values of the precipitation ($\delta^{18}O_{precip}$) from which they formed (Lachniet, 2009). A recent study (Moseley et al., 2021) used high-arctic speleothems to provide first approximations of Greenland precipitation $\delta^{18}O$ values for MIS 13–15 (~500–600 ka) by measuring stable isotopes at 150-µm resolution. In addition, studies examining the simple presence or absence of high-latitude speleothem growth in past interglacials have suggested a marked increase in permafrost persistence after MIS 11 in both Siberia and northwestern Canada (Biller-Celander et al., 2021; Vaks et al., 2013, 2020).

Annual bands can also often be identified in speleothems using various methods, such as confocal laser fluorescent microscopy (CLFM) (Batchelor et al., 2023; Orland et al., 2009). These bands are manifested as bright-to-dark fluorescent couplets that range from µm to mm in thickness. Their fluorescent properties are a result of large seasonal variations of organic acid load carried by dripwater, which is caused by strong seasonal climate regimes. The seasonality at a given location likely controls the timing of fluorescent band formation. Secondary Ion Mass Spectrometry (SIMS) can be employed to measure $\delta^{18}O$ at ultra-high-resolution across fluorescent annual bands (e.g., Baldini et al., 2021; Batchelor et al., 2022). These combined methods allow the reconstruction of past seasonal variations in cave dripwaters and temperatures.

In this study, we dated six speleothems, or more specifically, flowstones, from a cave in Northwest Territories (NWT), Canada (Figure 1a; Supporting Information S1) with U-Th methods to growth periods that occurred during three of the last four interglacial periods—Marine Isotope Stages (MIS) 11, 9, and substage 5e. After constructing age models for each sample (Figures S1–S6 in Supporting Information S1), we applied a two-tiered methodological approach to reconstruct past subarctic climate. First, we produce an ultra-high-resolution $\delta^{18}O$ record that, although not continuous, spans thousands of years for portions of these interglacials. This record was created using SIMS to measure $\delta^{18}O$ approximately every 35-µm down each sample's growth axis. Second, we used CLFM to identify several fluorescent annual bands in each speleothem, which we then targeted for additional SIMS measurements (Figures S7 and S8 in Supporting Information S1). Though these subarctic speleothems are small in size (most are <10 cm in length), the application of both CLFM and SIMS on these samples demonstrate their potential for providing ultra-high-resolution records of high-latitude Northern Hemisphere terrestrial climate outside of Greenland and provide insights into interpretive frameworks for future cold-region speleothem $\delta^{18}O$ records.

2. Modern Cave Setting and Climatology

The speleothems analyzed in this study were collected from Grotte Valerie (GV) cave (Figure S9 in Supporting Information S1), located in the Nahanni Plateau region of NWT, Canada (61.3°N, 124.1°W, 700–740 m [m] a.s.l.; Figure 1a) in Nahanni National Park Reserve (Parks Canada Agency, 2023). The cave has over 2,000 m of mapped passageways and has a maximum overburden of 50 m (Biller-Celander et al., 2021; Ford, 1973). This region is characterized by discontinuous permafrost (Brook, 1976; Yonge et al., 2018) (Text S1 in Supporting Information S1). Five regional GNIP sites (Figure 1a) are the closest precipitation monitoring stations to the GV cave system. Averaged monthly climate data from these sites (Figure 1b) highlight the extreme continental climate of this region with very large differences between average winter (December-February; −19°C) and summer (June-August 14°C) temperatures (IAEA/WMO, 2021). Average monthly temperatures remain below 0° C from November through March. The data also reveal that modern precipitation averages 300 mm/year, with most precipitation falling in summer, and that $\delta^{18}O_{precip}$ is strongly seasonal, with the highest $\delta^{18}O_{precip}$ values observed in summer (−17‰, VSMOW) and the lowest values present in winter (−27 ‰, VSMOW) (Figure 1b). The modern annual amount-weighted $\delta^{18}O_{precip}$ value from these sites is estimated to be −21‰ VSMOW.

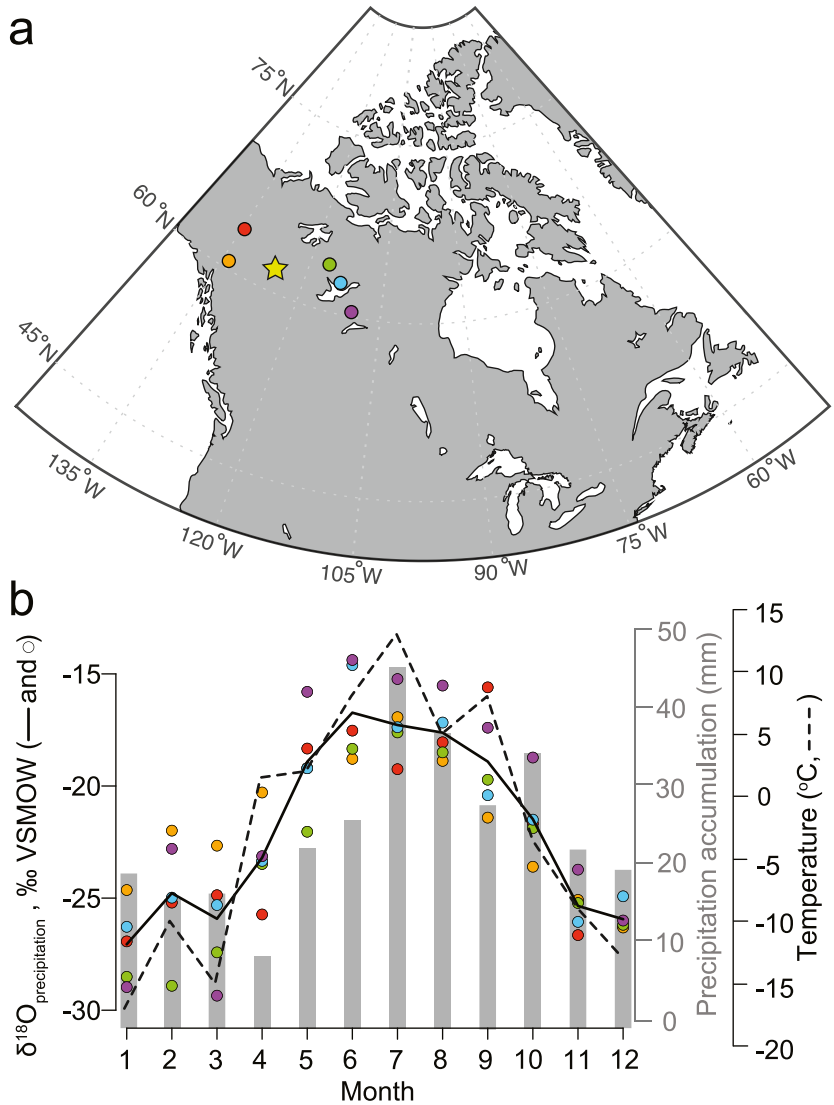

Figure 1. Map of study region with modern monthly precipitation isotopes ($\delta^{18}O_{precip}$). (a) Map of Canada with Grotte Valerie cave (yellow star). The location of the five closets Global Network of Isotopes in Precipitation (GNIP) stations (Fort Smith, Alberta [purple, 670 km from GV]; Snare Rapids, NWT [green, 480 km from GV]; Whitehorse, Yukon [orange, 590 km from GV]; Yellowknife, NWT [blue, 530 km from GV]; and Mayo, Yukon [red, 625 km from GV]) is also shown. (b) Monthly precipitation oxygen isotope ($\delta^{18}O_{precip}$) data for each GNIP station. Average monthly $\delta^{18}O_{precip}$ from all station data is also shown (solid black line). The color of the dots in the monthly precipitation data match the location of the GNIP station. Monthly temperature (dashed black line) and precipitation accumulation amount (gray bars) from the Yellowknife station (blue) is also shown.

3. Results

U-Th ages of GV speleothems (Text S2 in Supporting Information S1) span portions of MIS 11, 9, 7, and 5e (Data Set S1 in https://arcticdata.io/catalog/view/doi:10.18739/A2SJ19S7M; Figure 2a; Figure S10 in Supporting Information S1). These ages were used to produce age models of growth (Ramsey & Lee, 2013); we did not produce an age model for MIS 7 deposits because we identified only one ∼2 mm-thick layer accompanied by a single age from this interglacial. The specific growth periods as deduced from these age models (Figure 2b) across each interglacial are 409–376 ka (MIS 11), 336–305 ka (MIS 9), and 123–118 ka (MIS 5e). We used these age models to produce $\delta^{18}O$ time series across each interglacial.

10.1029/2024GL108459

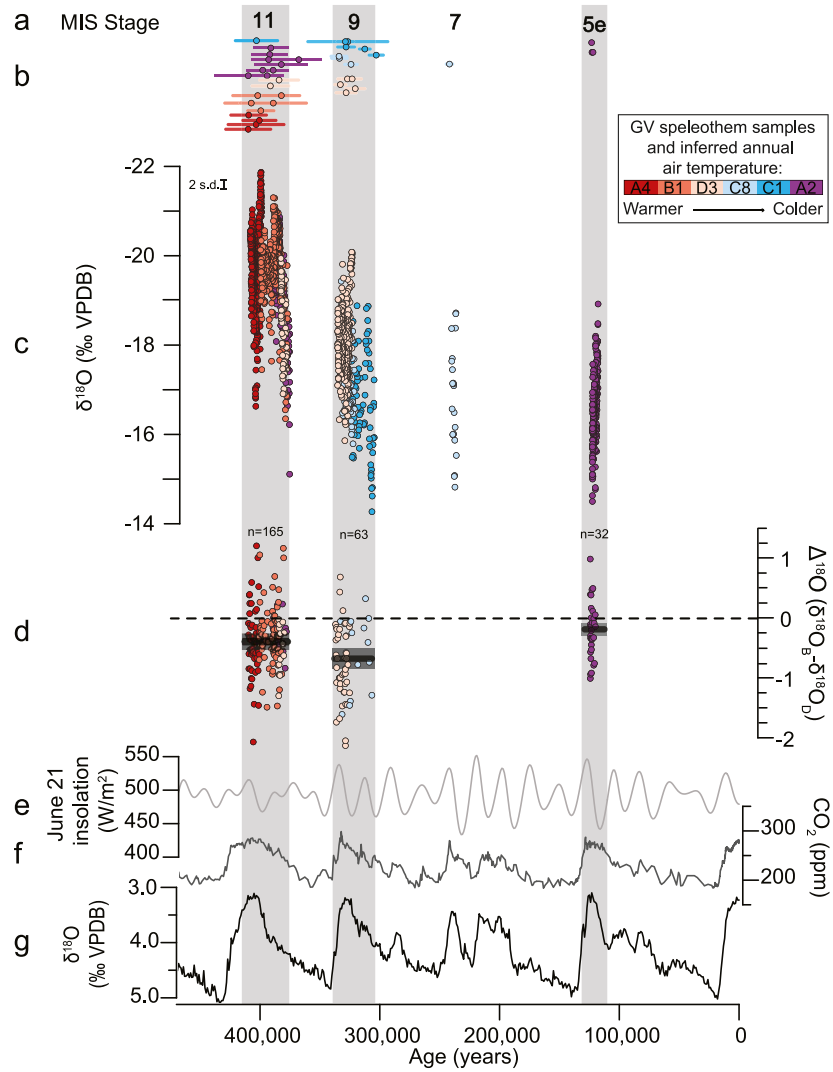

Figure 2. Paleoclimate data from GV speleothems in comparison with global climate records. (a) Labeled Marine Isotope Stages (MIS). (b) Uranium-Thorium dates from GV speleothems with associated 2 s.d. errors. (c) SIMS oxygen isotope ($\delta^{18}O$) data. Note the *y*-axis is flipped. (d) Intra-band ($\Delta^{18}O$) data from annual growth bands, with mean values (black lines) and standard errors of the mean (gray shading). The number of annual bands analyzed in each MIS stage is labeled in "$n = \#$." (e) June 21 insolation (W/m^2) from 61°N (Laskar et al., 2004). (f) CO_2 concentration (ppm) (EPICA community members, 2004). (g) Benthic $\delta^{18}O$ data (Lisiecki & Raymo, 2005). Colored data represent different speleothems and inferred annual air temperatures, which are deduced from our preferred interpretation that GV $\delta^{18}O$ reflects regional cooling from shorter annual ground thaw durations from MIS 11 to MIS 5e.

A total of 1663 SIMS $\delta^{18}O$ measurements with an average precision of 0.23‰ (2 sd, Data Set S2, https://arcticdata.io/catalog/view/doi:10.18739/A2SJ19S7M) were made across the six samples (Data Sets S2 and S3 in https://arcticdata.io/catalog/view/doi:10.18739/A2SJ19S7M) and reveal different average $\delta^{18}O$ signatures between interglacial periods (Figure 2c). The MIS 11 portion of the $\delta^{18}O$ record spans the longest time interval (~30 kyr) and extends late into the interglacial, featuring a distinct increase of $\delta^{18}O$ values when global climate records indicate cooling associated with the MIS 11-10 transition. A breakpoint analysis (Figure S11c in Supporting Information S1) identifies the end of peak-interglacial conditions at ~384 ka in our record. The average $\delta^{18}O$ value during peak MIS 11 conditions in our record (e.g., 409–384 ka) is −19.8‰ (±0.03 standard error of the mean, or "std. error"). $\delta^{18}O$ values increase in subsequent interglacials, with an average $\delta^{18}O$ value for MIS 9 speleothems of −17.7‰ (±0.05‰), −16.7‰ (±0.25‰) for MIS 7, and –16.6‰ (±0.05‰) for MIS 5e speleothems (Figure 2c).

10.1029/2024GL108459

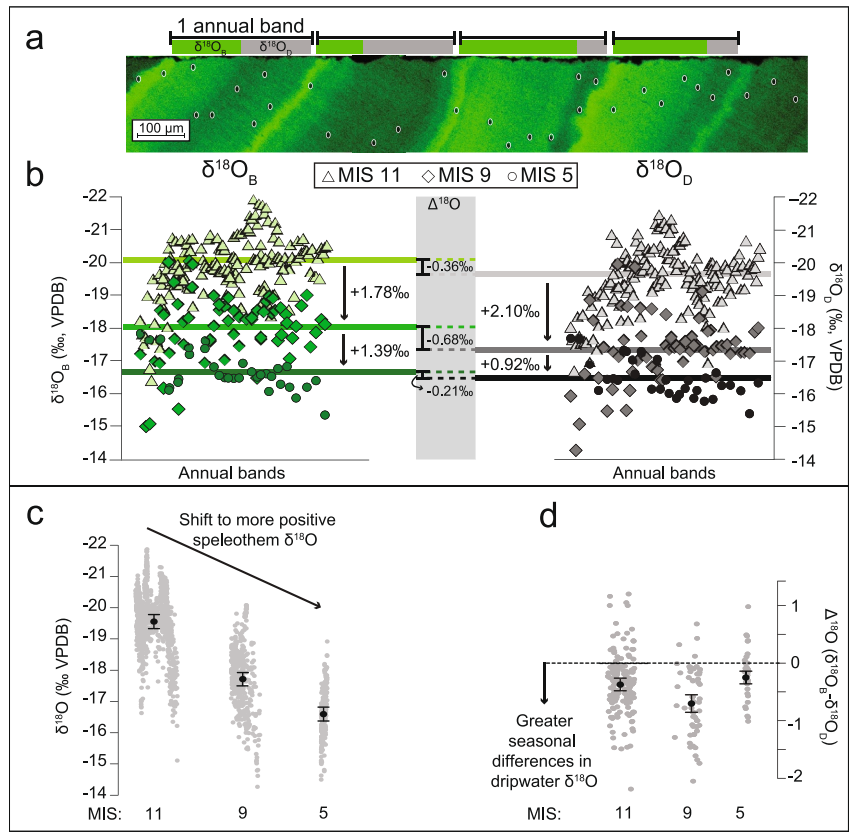

Figure 3. Results of seasonal oxygen isotope ($\delta^{18}O$) values within annual bands of GV speleothems and inferred seasonal cycle of ground thaw/freeze. (a) CLFM image of annual bands in a GV speleothem that shows intra-band SIMS analysis pits (white circles) measured across bright ($\delta^{18}O_B$) and dark ($\delta^{18}O_D$) fluorescent zones. (b) Values of $\delta^{18}O_B$ (left) and $\delta^{18}O_D$ (right) with annual bands of GV speleothems that grew during MIS 11 (triangles), 9 (diamonds), and 5 (circles). Values of $\Delta^{18}O$ ($\delta^{18}O_B$-$\delta^{18}O_D$) for each interglacial are also shown (middle gray shading). (c) SIMS $\delta^{18}O$ values of MIS 11, 9, and 5 (gray dots), with average values (black dots) and 2 standard errors of the mean (std error). (d) Intra-band $\Delta^{18}O$ data (with means and ±2 std error), interpreted as differences in the relative proportion of seasonal precipitation as dripwater.

CLFM imaging reveals distinct fluorescent banding throughout each sample (Figure S8 in Supporting Information S1) (Baker et al., 2021). Annual growth bands were identified as couplets including one bright zone and an adjacent dark zone (Figure 3a). As many fluorescent bands are thinner than the ~5–10 µm spatial resolution of the SIMS (<5-µm thick), "we targeted individual annual bands that ranged from 6 to 407 µm in thickness (average 70-µm) for intra-band $\delta^{18}O$ measurements (Data Set S3, https://arcticdata.io/catalog/view/doi:10.18739/A2SJ19S7M)" to resolve differences in $\delta^{18}O$ of bright ($\delta^{18}O_B$) and dark ($\delta^{18}O_D$) zones to infer past seasonal climate conditions (MIS 11: $n = 165$, MIS 9: $n = 63$, MIS 5: $n = 32$) (Figures 3a and 3b). The average value of $\delta^{18}O_B$ is typically lower than $\delta^{18}O_D$ within annual bands. The average values of $\delta^{18}O_B$ and $\delta^{18}O_D$ are also statistically different between interglacial periods, as determined by a Kolmogorov-Smirnov statistical test (Massey, 1951). The average values of both $\delta^{18}O_B$ and $\delta^{18}O_D$ increase from older to younger interglacial periods ($\delta^{18}O_B$ of peak MIS 11 = −20.1‰, $\delta^{18}O_B$ of MIS 9 = −18.1‰, $\delta^{18}O_B$ of MIS 5e = −16.7‰; $\delta^{18}O_D$ of peak MIS 11 = −19.8‰, $\delta^{18}O_D$ of MIS 9 = −17.4‰, $\delta^{18}O_D$ of MIS 5e = −16.6‰) (Figure 3b). The average differences between $\delta^{18}O_B$ and $\delta^{18}O_D$ within individual annual bands, referred to here as $\Delta^{18}O$ values ($\delta^{18}O_B$-$\delta^{18}O_D$), are negative for all MIS stages, but vary in magnitude. The average $\Delta^{18}O$ signature of MIS 11 speleothems is −0.36‰ (±0.04‰ std. error), −0.68‰ (±0.09) for MIS 9 speleothems, and −0.21‰ (±0.08) for MIS 5e speleothems (Figures 2d and 3d).

4. Discussion

The most prominent result in our data set is a ~3‰ increase in mean $\delta^{18}O$ values in GV speleothems from MIS 11 to MIS 5e. Insolation does not seem to be an obvious driver of GV speleothem $\delta^{18}O$ because GV speleothem $\delta^{18}O$

trends across MIS 11-10 (Figure S11 in Supporting Information S1) follow the longer term structure of global climate evolution (e.g., benthic $\delta^{18}O$; Lisiecki & Raymo, 2005) with little apparent orbital (i.e., 20-kyr) variability (Laskar et al., 2004). Further, while MIS 5e had higher peak summer insolation than MIS 11 (Laskar et al., 2004), our sample dates to 123–118 ka, which occurs well after the peak and at a time when summer insolation was near average MIS 11 values (Figure 2e). We therefore explore other potential interpretations for this increase, taking into account the different climatic factors (Fairchild et al., 2006; Lachniet, 2009), including changes in precipitation patterns and/or temperature, that affect speleothem $\delta^{18}O$.

We first consider how changes in mean annual air temperature (MAAT) might have affected $\delta^{18}O$ in the GV speleothem record. At high-latitudes, changes in MAAT result in changes in $\delta^{18}O_{precip}$, with higher (lower) $\delta^{18}O_{precip}$ values associated with warmer (colder) conditions. This temperature effect on $\delta^{18}O_{precip}$ is, on average, 0.7‰ $°C^{-1}$ (Dansgaard, 1964). However, temperature also drives an opposing effect on the $\delta^{18}O$ of speleothem calcite during formation with a magnitude of −0.18 to −0.24‰ $°C^{-1}$ (Kim & O'Neil, 1997); These two effects are typically coupled, such that the combined influence of changes in MAAT on speleothem calcite $\delta^{18}O$ values is roughly 0.5‰ $°C^{-1}$. If we interpret the GV speleothem $\delta^{18}O$ record in terms of only these two factors, the 3‰ increase from MIS 11 to MIS 5e would imply that MIS 5e was ∼6°C warmer than MIS 11 in NWT.

This interpretation is unlikely, as global paleoclimate records indicate MIS 11 to be one of the warmest interglacials of the last 800 ka (Past Interglacials Working Group of PAGES, 2016). High-latitude paleoclimate records from the Northern Hemisphere (Minyuk et al., 2014; Snyder et al., 2013), including Greenland (de Vernal & Hillaire-Marcel, 2008; Irvalı et al., 2020) and northern Siberia (Melles et al., 2012), suggest MIS 11 was a period of extreme warmth. Speleothem growth histories, including from the NWT, suggest that MIS 11 was marked by broader permafrost degradation than any subsequent interglacial (Biller-Celander et al., 2021; Vaks et al., 2013). We also measured the amount of carbonate growth in between U-Th ages in each GV speleothem and found that the total amount of accumulated growth at our cave site is highest during MIS 11 at 89 mm, yet only 14.5 and 6 mm in MIS 9 and MIS 5e, respectively (Figure S12 in Supporting Information S1). Higher speleothem growth rates have been linked to warmer and wetter climates (Railsback, 2018). Even accounting for the longer duration of growth recorded during MIS 11, MIS 5e was marked by a factor of ∼2 lower growth rate in our samples. A previous study that dated several other speleothems from GV and other caves in Nahanni National Park Reserve found five samples from MIS 11, including a 14 cm stalagmite, and no samples dating to MIS 5 (Biller-Celander et al., 2021).

We also observe an inverse relationship between $\delta^{18}O$ and temperatures in the structure of our speleothem $\delta^{18}O$ record across MIS 11, as average $\delta^{18}O$ values increase by 2‰ near the end of MIS 11 when other paleoclimate records (Lisiecki & Raymo, 2005) indicate global cooling (Figure 2; Figure S11 in Supporting Information S1). This relationship would suggest lower speleothem $\delta^{18}O$ values reflect warmer temperatures in GV speleothems, which is opposite to our positive estimation of 0.5‰ $°C^{-1}$ above. We therefore suggest that direct temperature effects are likely not the primary factor contributing to $\delta^{18}O$ variability in the GV speleothem record and consider three other possibilities: (a) changes in the ratio of winter to summer precipitation; (b) changes in moisture source; and (c) changes in the contribution of winter precipitation to dripwaters.

Speleothem $\delta^{18}O$ values can be affected by changes in the relative proportion of seasonal precipitation. As stated previously, the strongly seasonal climate of NWT Canada causes a distinct cycle of $\delta^{18}O_{precip}$, with cold-season $\delta^{18}O_{precip}$ nearly 10‰ lower than warm-season $\delta^{18}O_{precip}$. This large seasonal variability of $\delta^{18}O_{precip}$ means that changes in the relative contribution of seasonal precipitation to dripwater can easily affect speleothem $\delta^{18}O$. Using modern seasonal $\delta^{18}O_{precip}$ patterns, we find that only a 10% increase in the proportion of winter precipitation and a corresponding 10% decrease in the proportion of summer precipitation would decrease amount-weighted-$\delta^{18}O_{precip}$ values by nearly 1‰.

Under this scenario, the low-$\delta^{18}O$ signature of MIS 11 speleothems could reflect increased cold-season (e.g., winter) precipitation, and a decreasing fraction of cold-season precipitation from MIS 11 to MIS 5e caused successively higher speleothem calcite $\delta^{18}O$ values. Consistent with this hypothesis, simulations of 21st century warming and sea ice loss show substantial increases in winter precipitation amount and in the fraction of precipitation that falls in the cold season in the Arctic and parts of the subarctic (Deser et al., 2010). In addition, Miocene tree rings from northern Siberia reflecting a warmer climate show evidence for increased winter precipitation fraction (Schubert et al., 2017). As 21st century warming and Miocene climate may not adequately reflect conditions during Pleistocene interglacials, we examined the contribution of winter precipitation and mean

annual average temperature at our field site (61°N, 124°W) in a recent transient coupled general circulation model simulation spanning the last 3 Ma (Timmermann et al., 2022). We found a negative correlation between mean annual temperature and winter precipitation fraction in warm climates of the last 3 Ma (Figure S13 in Supporting Information S1), inconsistent with the hypothesis that warmer temperatures in MIS 11 were associated with an increase in the proportion of winter precipitation. While it remains possible that increased cold-season precipitation was the cause of the low $\delta^{18}O$ values of MIS 11 speleothems, further work will be needed to test this hypothesis.

A second potential cause of low $\delta^{18}O$ values in MIS 11 GV speleothems is a change in moisture sources. Modeling studies suggest that shifts in evaporative source areas within the North Pacific associated with interannual to decadal ocean-atmosphere variability can drive changes in $\delta^{18}O_{precip}$ of up to several per mil in Canada (Anderson et al., 2016; Field et al., 2010), and ice core $\delta^{18}O$ records from the region are commonly interpreted as reflecting atmospheric circulation (Aleutian Low strength) rather than temperature (Field et al., 2010). Persistent differences in atmospheric circulation during MIS 11 may therefore have delivered more depleted moisture to the cave site. More speculatively, perhaps a larger share of precipitation was sourced from outside the Pacific basin during MIS 11. In the present day, moisture originating from the Arctic Ocean has lower $\delta^{18}O$ values than moisture originating from the midlatitudes (Mellat et al., 2021) and observational evidence suggests that recent declines in Arctic sea ice have been accompanied by increases in Arctic-sourced moisture in Northern Hemisphere high-latitude precipitation (Kopec et al., 2016). It is therefore possible that reduced sea ice in MIS 11 (Cronin et al., 2013) would have led to more Arctic-sourced moisture supplying precipitation to northwestern Canada, lowering $\delta^{18}O_{precip}$ values despite warmer conditions, though we view this possibility as unlikely due to the prevailing southwesterly storm tracks in this region.

A final factor we consider that may affect GV speleothem $\delta^{18}O$ variability between interglacials is seasonal filtering of infiltration due to changes in the duration of annual ground thaw. In cold regions, winter snow that melts prior to ground thaw runs off rather than infiltrating (Pavoni et al., 2022). Colder periods would cause a decrease in the contribution of winter precipitation as dripwater because prolonged freezing ground conditions would limit the amount of lowest-$\delta^{18}O_{precip}$ cold-season precipitation contributing to dripwaters. This process is independent of changes in the ratio of winter to summer precipitation, the first scenario we posed.

Under this scenario, we interpret $\delta^{18}O$ values in the GV speleothem record to reflect changes in past temperatures through their influence on how long throughout the year the overlying ground surface remains frozen or is thawed (i.e., the length of the frost season) (Yonge et al., 2018). Lower speleothem calcite $\delta^{18}O$ values would then correlate with warmer annual air temperatures, as the longer duration of annual ground thaw would result in an increased contribution of cold-season precipitation to cave dripwater. Conversely, higher speleothem calcite $\delta^{18}O$ signatures would correlate with colder annual temperatures when the duration of annual ground thaw is relatively short due to a decreased contribution of cold-season precipitation to dripwater. This mechanism has been invoked to explain speleothem records from Sweden that also show lower $\delta^{18}O$ signatures during warmer periods (MIS 5e vs. MIS 1) (Finné et al., 2019; Sundqvist et al., 2007).

After considering the mechanisms above, we suggest that the shift toward higher $\delta^{18}O$ values in more recent interglacials is most likely due to a reduction in the duration of seasonal ground thaw from MIS 11 to MIS 9 and 5 in response to regional cooling in northwestern Canada across this time (Figure 2c). An increasing duration of the frost season reduced the amount of low-$\delta^{18}O$ cold-season precipitation entering the karst aquifer, resulting in high dripwater $\delta^{18}O$ values. We suggest that this mechanism also explains the +2 ‰ increase of our speleothem $\delta^{18}O$ record across the MIS 11-10 transition (Figure S11 in Supporting Information S1). This interpretation is consistent with a previous study that linked decreasing calcite precipitation after MIS 11 across cave systems in northwest Canada with increased permafrost persistence (Biller-Celander et al., 2021). It is also consistent with the reduced amount of calcite precipitated in GV during MIS 9 and 5e relative to MIS 11. However, we cannot rule out an increase in the amount of cold-season precipitation or a change in moisture source as potential drivers of low GV $\delta^{18}O$ values in MIS 11, and it is likely that multiple mechanisms acted in concert.

Finally, we discuss the intra-band analyses. We find that differences between $\delta^{18}O$ values of bright zones ("$\delta^{18}O_B$") and dark zones ("$\delta^{18}O_D$") are small and relatively consistent between interglacials, averaging −0.36‰ in MIS 11, −0.68‰ in MIS 9, and −0.21‰ in MIS 5. The consistency and small magnitude of intra-band $\delta^{18}O$ changes in all GV speleothems attests to the relatively stable cave environment. Our interpretation that fluorescent bands in GV speleothems record annual variations of climate is supported by the finding that $\delta^{18}O_B$ values are

consistently lower than $\delta^{18}O_D$ values. Negative $\Delta^{18}O$ values mirror the seasonal $\delta^{18}O_{precip}$ cycle in NWT Canada, where cold-season $\delta^{18}O_{precip}$ values are much lower than warm-season $\delta^{18}O_{precip}$ (Figure 1b). We propose that this seasonal climate cycle in subarctic Canada increases organic acid load during the spring thaw (bright bands) and decreases organic acid load in the summer (dark bands) (Figure S15 in Supporting Information S1). We also observe that MIS 5e speleothems have the highest and closest to zero $\Delta^{18}O$ signature compared to speleothems from the other two interglacials. One way to interpret near-zero $\Delta^{18}O$ values is that bright and dark zones formed from dripwater derived from precipitation with similar $\delta^{18}O_{precip}$. Under this scenario, the near-zero $\Delta^{18}O$ values in MIS 5e are consistent with a reduced seasonal duration of ground thaw from a longer frost season, which would result in calcite precipitation primarily only occurring in the warmer months from warm-season dripwater with similar $\delta^{18}O_{precip}$ signatures. Conversely, the more-negative $\Delta^{18}O$ signatures in MIS 11 and 9 compared to MIS 5e may suggest that winter/spring precipitation more frequently infiltrated the cave as dripwater due to longer periods of seasonal ground thaw and a shorter frost season.

5. Conclusions

In this study, we analyzed six subarctic Canada speleothems that grew across three former interglacial periods to provide an ultra-high-resolution record of high-latitude climate that is beyond the current range of Northern Hemisphere ice cores. We find that average $\delta^{18}O$ values in these samples increased by 3‰ from MIS 11 to MIS 5e, which we interpret as reflecting a decrease in the infiltration of cold-season precipitation due to regional cooling that shortened seasonal ground thaw durations in subsequent interglacials. In addition, decreased sea ice in MIS 11 may have enhanced the fraction of cold-season precipitation and/or shifted the moisture source for precipitation into northwestern Canada, lowering $\delta^{18}O_{precip}$. Results from our intra-band analyses add to our interpretation of the records, supporting the existence of annual bands and relatively consistent cave environments marked by small seasonal temperature changes. The close-to-0‰ $\Delta^{18}O$ signature of MIS 5e speleothems is consistent with reduced duration of seasonal ground thaw, while lower $\Delta^{18}O$ values in MIS 9 and MIS 11 speleothems suggest greater infiltration of winter/spring precipitation.

This study shows the potential of subarctic speleothems to extend the ultra-high-resolution isotopic records of past climate traditionally obtained from ice cores to earlier interglacials. Our results also demonstrate how high-latitude speleothems record changes in climate differently than the direct precipitation archives from ice cores. In particular, speleothem $\delta^{18}O$ appears sensitive to changes in the duration of annual ground thaw through its effect on relative contribution of seasonal precipitation to the groundwater budget. Overall, this study highlights the utility in the development of records of past climate beyond both the geographic and temporal limitations of ice cores, which will better our understanding of past climate conditions. The development of more ultra-high-resolution interglacial speleothem records in high latitudes will test our results and help to refine the interpretive framework presented here, and ultimately reveal how parts of the Arctic system respond to warming at the shorter timescales of most relevance to society.

Data Availability Statement

All data needed to evaluate the conclusions in this paper are available in Batchelor et al. (2024), https://arcticdata.io/catalog/view/doi:10.18739/A2SJ19S7M.

Acknowledgments
This work is supported by the National Science Foundation (AGS-2052633 to C.J. B.; OPP-2103100 to D.M., OPP-2109039 to J.D.S.). Sample collection in 2019 was supported by the mTerra Catalyst Fund at MIT. We thank Parks Canada, Dave Critchley of Northern Alberta Institute of Technology, WiscSIMS Laboratory, Optical Imaging Core at UW-Madison, and the Stable Isotope Laboratory at Northwestern University. We also thank Axel Timmermann for providing access to climate model output that contributed to the study.

References

Anderson, L., Berkelhammer, M., Barron, J. A., Steinman, B. A., Finney, B. P., & Abbott, M. B. (2016). Lake oxygen isotopes as recorders of North American Rocky Mountain hydroclimate: Holocene patterns and variability at multi-decadal to millennial time scales. *Global and Planetary Change*, *137*, 131–148.

Baker, A., Mariethoz, G., Comas-Bru, L., Hartmann, A., Frisia, S., Borsato, A., et al. (2021). The properties of annually laminated Stalagmites-A global synthesis. *Reviews of Geophysics*, *59*(2), e2020RG000722. https://doi.org/10.1029/2020rg000722

Baldini, J. U., Lechleitner, F. A., Breitenbach, S. F., van Hunen, J., Baldini, L. M., Wynn, P. M., et al. (2021). Detecting and quantifying palaeoseasonality in stalagmites using geochemical and modelling approaches. *Quaternary Science Reviews*, *254*, 106784. https://doi.org/10.1016/j.quascirev.2020.106784

Batchelor, C. J., Marcott, S. A., Orland, I. J., He, F., & Edwards, R. L. (2023). Decadal warming events extended into central North America during the last glacial period. *Nature Geoscience*, *16*(3), 257–261. https://doi.org/10.1038/s41561-023-01132-3

Batchelor, C. J., Marcott, S. A., Orland, I. J., & Kitajima, K. (2022). Late Holocene increase of winter precipitation in mid-continental North America from a seasonally resolved speleothem record. *Geology*, *50*(7), 781–785. https://doi.org/10.1130/g50096.1

Batchelor, C. J., McGee, D., Shakun, J. D., Woodhead, J. D., Jost, A. B., Arnold, S., et al. (2024). Uranium-Thorium ages and stable oxygen isotope data on speleothems that grew during Marine Isotope Stages (MIS) 11, 9, and MIS 5e, Northwest Territories, Canada. [Dataset]. *Arctic Data Center*. https://doi.org/10.18739/A2SJ19S7M

Biller-Celander, N., Shakun, J. D., McGee, D., Wong, C. I., Reyes, A. V., Hardt, B., et al. (2021). Increasing Pleistocene permafrost persistence and carbon cycle conundrums inferred from Canadian speleothems. *Science Advances*, *7*(18), eabe5799. https://doi.org/10.1126/sciadv.abe5799

Brook, A. G. (1976). Geomorphology of the North Karst, South Nahanni River region, Northwest Territories, Canada. (PhD Thesis).

Cheng, H., Edwards, R. L., Shen, C.-C., Polyak, V. J., Asmerom, Y., Woodhead, J., et al. (2013). Improvements in ^{230}Th dating, ^{230}Th and ^{234}U half-life values, and U–Th isotopic measurements by multi-collector inductively coupled plasma mass spectrometry. *Earth and Planetary Science Letters*, *371*, 82–91. https://doi.org/10.1016/j.epsl.2013.04.006

Clark, P. U., Shakun, J. D., Rosenthal, Y., Köhler, P., & Bartlein, P. J. (2024). Global and regional temperature change over the past 4.5 million years. *Science*, *383*(6685), 884–890. https://doi.org/10.1126/science.adi1908

Cluett, A. A., & Thomas, E. K. (2021). Summer warmth of the past six interglacials on Greenland. *Proceedings of the National Academy of Sciences*, *118*(20), e2022916118. https://doi.org/10.1073/pnas.2022916118

Cronin, T. M., Polyak, L., Reed, D., Kandiano, E. S., Marzen, R. E., & Council, E. A. (2013). A 600-ka Arctic sea-ice record from Mendeleev Ridge based on ostracodes. *Quaternary Science Reviews*, *79*, 157–167. https://doi.org/10.1016/j.quascirev.2012.12.010

Dansgaard, W. (1964). Stable isotopes in precipitation. *Tellus*, *16*(4), 436–468. https://doi.org/10.3402/tellusa.v16i4.8993

Deser, C., Tomas, R., Alexander, M., & Lawrence, D. (2010). The seasonal atmospheric response to projected Arctic sea ice loss in the late twenty-first century. *Journal of Climate*, *23*(2), 333–351. https://doi.org/10.1175/2009jcli3053.1

de Vernal, A., & Hillaire-Marcel, C. (2008). Natural variability of Greenland climate, vegetation, and ice volume during the past million years. *Science*, *320*(5883), 1622–1625. https://doi.org/10.1126/science.1153929

EPICA community members. (2004). Eight glacial cycles from an Antarctic ice core. *Nature*, *429*(6992), 623–628. https://doi.org/10.1038/nature02599

Fairchild, I. J., Smith, C. L., Baker, A., Fuller, L., Spötl, C., Mattey, D., & McDermott, F. (2006). Modification and preservation of environmental signals in speleothems. *Earth-Science Reviews*, *75*(1), 105–153. https://doi.org/10.1016/j.earscirev.2005.08.003

Field, R. D., Moore, G. W. K., Holdsworth, G., & Schmidt, G. A. (2010). A GCM-based analysis of circulation controls on δ^{18}O in the southwest Yukon, Canada: Implications for climate reconstructions in the region. *Geophysical Research Letters*, *37*(5), 2009GL041408. https://doi.org/10.1029/2009GL041408

Finné, M., Salonen, S., Frank, N., Helmens, K. F., Schröder-Ritzrau, A., Deininger, M., & Holzkämper, S. (2019). Last interglacial climate in northern Sweden—Insights from a speleothem record. *Quaternary*, *2*(3), 29. https://doi.org/10.3390/quat2030029

Ford, D. C. (1973). Development of the canyons of the South Nahanni River, NWT. *Canadian Journal of Earth Sciences*, *10*(3), 366–378. https://doi.org/10.1139/e73-033

IAEA/WMO. (2021). Global network of isotopes in precipitation. Retrieved from http://www.iaea.org/water

Irvalı, N., Galaasen, E. V., Ninnemann, U. S., Rosenthal, Y., Born, A., & Kleiven, H. (2020). A low climate threshold for south Greenland Ice Sheet demise during the Late Pleistocene. *Proceedings of the National Academy of Sciences of the United States of America*, *117*(1), 190–195. https://doi.org/10.1073/pnas.1911902116

Kim, S.-T., & O'Neil, J. R. (1997). Equilibrium and nonequilibrium oxygen isotope effects in synthetic carbonates. *Geochimica et Cosmochimica Acta*, *61*(16), 3461–3475. https://doi.org/10.1016/s0016-7037(97)00169-5

Kopec, B. G., Feng, X., Michel, F. A., & Posmentier, E. S. (2016). Influence of sea ice on Arctic precipitation. *Proceedings of the National Academy of Sciences of the United States of America*, *113*(1), 46–51. https://doi.org/10.1073/pnas.1504633113

Lachniet, M. S. (2009). Climatic and environmental controls on speleothem oxygen-isotope values. *Quaternary Science Reviews*, *28*(5–6), 412–432. https://doi.org/10.1016/j.quascirev.2008.10.021

Laskar, J., Robutel, P., Joutel, F., Gastineau, M., Correia, A. C. M., & Levrard, B. (2004). A long-term numerical solution for the insolation quantities of the Earth. *Astronomy & Astrophysics*, *428*(1), 261–285. https://doi.org/10.1051/0004-6361:20041335

Lisiecki, L. E., & Raymo, M. E. (2005). A Pliocene-Pleistocene stack of 57 globally distributed benthic δ^{18}O records. *Paleoceanography*, *20*(1). https://doi.org/10.1029/2004pa001071

Massey, F. J., Jr. (1951). The Kolmogorov-Smirnov test for goodness of fit. *Journal of the American Statistical Association*, *46*(253), 68–78. https://doi.org/10.2307/2280095

Mellat, M., Bailey, H., Mustonen, K.-R., Marttila, H., Klein, E. S., Gribanov, K., et al. (2021). Hydroclimatic controls on the isotopic (δ^{18}O, δ^{2}H, d-excess) traits of Pan-Arctic summer rainfall events. *Frontiers in Earth Science*, *9*, 651731. https://doi.org/10.3389/feart.2021.651731

Melles, M., Brigham-Grette, J., Minyuk, P. S., Nowaczyk, N. R., Wennrich, V., DeConto, R. M., et al. (2012). 2.8 million years of Arctic climate change from Lake El'gygytgyn, NE Russia. *Science*, *337*(6092), 315–320. https://doi.org/10.1126/science.1222135

Minyuk, P. S., Borkhodoev, V. Y., & Wennrich, V. (2014). Inorganic geochemistry data from Lake El'gygytgyn sediments: Marine isotope stages 6–11. *Climate of the Past*, *10*(2), 467–485. https://doi.org/10.5194/cp-10-467-2014

Moseley, G. E., Edwards, R. L., Lord, N. S., Spötl, C., & Cheng, H. (2021). Speleothem record of mild and wet mid-Pleistocene climate in northeast Greenland. *Science Advances*, *7*(13), eabe1260. https://doi.org/10.1126/sciadv.abe1260

NGRIP members. (2004). High-resolution record of Northern Hemisphere climate extending into the last interglacial period. *Nature*, *431*(7005), 147–151. https://doi.org/10.1038/nature02805

Orland, I. J., Bar-Matthews, M., Kita, N. T., Ayalon, A., Matthews, A., & Valley, J. W. (2009). Climate deterioration in the Eastern Mediterranean as revealed by ion microprobe analysis of a speleothem that grew from 2.2 to 0.9 ka in Soreq Cave, Israel. *Quaternary Research*, *71*(1), 27–35. https://doi.org/10.1016/j.yqres.2008.08.005

Parks Canada Agency. (2023). Nahanni National Park Reserve. Retrieved from https://parks.canada.ca/pn-np/nt/nahann

Past Interglacials Working Group of PAGES. (2016). Interglacials of the last 800,000 years. *Reviews of Geophysics*, *54*(1), 162–219. https://doi.org/10.1002/2015RG000482

Pavoni, M., Boaga, J., Carrera, A., Zuecco, G., Carturan, L., & Zumiani, M. (2022). *Brief communication: Mountain permafrost acts as an aquiclude during an infiltration experiment monitored with ERT time-lapse measurements* (pp. 1–8). EGUsphere.

Pörtner, H.-O., Roberts, D. C., Adams, H., Adler, C., Aldunce, P., Ali, E., et al. (2022). In *Climate change 2022: Impacts, adaptation and vulnerability*. IPCC.

Railsback, L. B. (2018). A comparison of growth rate of late Holocene stalagmites with atmospheric precipitation and temperature, and its implications for paleoclimatology. *Quaternary Science Reviews*, *187*, 94–111. https://doi.org/10.1016/j.quascirev.2018.03.002

Ramsey, C. B., & Lee, S. (2013). Recent and planned developments of the program OxCal. *Radiocarbon*, *55*(2), 720–730. https://doi.org/10.2458/azu_js_rc.55.16215

Schubert, B. A., Jahren, A. H., Davydov, S. P., & Warny, S. (2017). The transitional climate of the late Miocene Arctic: Winter-dominated precipitation with high seasonal variability. *Geology*, *45*(5), 447–450. https://doi.org/10.1130/g38746.1

Snyder, J. A., Cherepanova, M. V., & Bryan, A. (2013). Dynamic diatom response to changing climate 0–1.2 Ma at lake El'gygytgyn, Far East Russian Arctic. *Climate of the Past*, *9*(3), 1309–1319. https://doi.org/10.5194/cp-9-1309-2013

Sundqvist, H. S., Holmgren, K., & Lauritzen, S.-E. (2007). Stable isotope variations in stalagmites from northwestern Sweden document climate and environmental changes during the early Holocene. *The Holocene*, *17*(2), 259–267. https://doi.org/10.1177/0959683607073292

Timmermann, A., Yun, K.-S., Raia, P., Ruan, J., Mondanaro, A., Zeller, E., et al. (2022). Climate effects on archaic human habitats and species successions. *Nature*, *604*(7906), 495–501. https://doi.org/10.1038/s41586-022-04600-9

Vaks, A., Gutareva, O. S., Breitenbach, S. F., Avirmed, E., Mason, A. J., Thomas, A. L., et al. (2013). Speleothems reveal 500,000-year history of Siberian permafrost. *Science*, *340*(6129), 183–186. https://doi.org/10.1126/science.1228729

Vaks, A., Mason, A. J., Breitenbach, S. F. M., Kononov, A. M., Osinzev, A. V., Rosensaft, M., et al. (2020). Palaeoclimate evidence of vulnerable permafrost during times of low sea ice. *Nature*, *577*(7789), 221–225. https://doi.org/10.1038/s41586-019-1880-1

Yonge, C. J., Ford, D., Horne, G., Lauriol, B., & Schroeder, J. (2018). Ice caves in Canada. In *Ice caves* (pp. 285–334). Elsevier.

References From the Supporting Information

Brotton, J., & Wall, G. (1997). Climate change and the Bathurst caribou herd in the Northwest Territories, Canada. *Climatic Change*, *35*(1), 35–52. https://doi.org/10.1023/a:1005313315265

Budikova, D., & Nkemdirim, L. C. (2005). Relative changes in consistency of winter surface air temperature during ENSO events across western Canada. *Canadian Geographies / Géographies Canadiennes*, *49*(1), 81–99. https://doi.org/10.1111/j.0008-3658.2005.00081.x

Dalzell, B. J., Filley, T. R., & Harbor, J. M. (2007). The role of hydrology in annual organic carbon loads and terrestrial organic matter export from a midwestern agricultural watershed. *Geochimica et Cosmochimica Acta*, *71*(6), 1448–1462. https://doi.org/10.1016/j.gca.2006.12.009

Edwards, R. L., Chen, J. H., & Wasserburg, G. J. (1987). $^{238}U^{234}U^{230}Th^{232}Th$ systematics and the precise measurement of time over the past 500,000 years. *Earth and Planetary Science Letters*, *81*(2–3), 175–192. https://doi.org/10.1016/0012-821x(87)90154-3

Emmerton, C. A., Lesack, L. F. W., & Marsh, P. (2007). Lake abundance, potential water storage, and habitat distribution in the Mackenzie River Delta, western Canadian Arctic. *Water Resources Research*, *43*(5), 2006WR005139. https://doi.org/10.1029/2006WR005139

Environment and Climate Change Canada Historical Climate Data. (2022). Environment and climate change Canada historical climate data [Dataset]. *Government of Canada*. Retrieved from https://climate.weather.gc.ca/index_e.html

Guo, L., Cai, Y., Belzile, C., & Macdonald, R. W. (2012). Sources and export fluxes of inorganic and organic carbon and nutrient species from the seasonally ice-covered Yukon River. *Biogeochemistry*, *107*(1–3), 187–206. https://doi.org/10.1007/s10533-010-9545-z

Kozdon, R., Ushikubo, T., Kita, N. T., & Valley, J. W. (2008). Intratest oxygen isotope variability in planktonic foraminifera: New insights from in situ measurements by ion microprobe. *Geochimica et Cosmochimica Acta - Supplement*, *72*(12), A496.

Orland, I. J., He, F., Bar-Matthews, M., Chen, G., Ayalon, A., & Kutzbach, J. E. (2019). Resolving seasonal rainfall changes in the Middle East during the last interglacial period. *Proceedings of the National Academy of Sciences of the United States of America*, *116*(50), 24985–24990. https://doi.org/10.1073/pnas.1903139116

Shabbar, A., Bonsal, B., & Khandekar, M. (1997). Canadian precipitation patterns associated with the Southern Oscillation. *Journal of Climate*, *10*(12), 3016–3027. https://doi.org/10.1175/1520-0442(1997)010<3016:cppawt>2.0.co;2

Spence, C., Kokelj, S. V., Kokelj, S. A., McCluskie, M., & Hedstrom, N. (2015). Evidence of a change in water chemistry in Canada's subarctic associated with enhanced winter streamflow. *Journal of Geophysical Research: Biogeosciences*, *120*(1), 113–127. https://doi.org/10.1002/2014JG002809

Whitfield, P. H., Moore, R. D., Fleming, S. W., & Zawadzki, A. (2010). Pacific decadal oscillation and the hydroclimatology of western Canada—Review and prospects. *Canadian Water Resources Journal*, *35*(1), 1–28. https://doi.org/10.4296/cwrj3501001